

Miscibility of Poly(sila- $\alpha$ -methylstyrene) with Polystyrene

Ralph-Dieter Maier, Jörg Kressler,\* Bernd Rudolf, Peter Reichert, Florian Koopmann, Holger Frey, and Rolf Mülhaupt

Institut für Makromolekulare Chemie und Freiburger Materialforschungszentrum, Albert-Ludwigs-Universität, Stefan-Meier-Strasse 21, D-79104 Freiburg i. Br., Germany

Received August 31, 1995; Revised Manuscript Received November 3, 1995<sup>⊗</sup>

**ABSTRACT:** The miscibility of the carbosilane analogue of poly( $\alpha$ -methylstyrene), poly(methylphenylsilylenemethylene), named poly(sila- $\alpha$ -methylstyrene) (PSi $\alpha$ MS) with an  $M_w$  value of 188 000 and polystyrene (PS) having different molecular weights is investigated using DSC and cloud point measurements. The observed miscibility behavior is described in terms of the Patterson equation-of-state theory using also PVT data of the respective polymers. Blends with polystyrene of an  $M_w$  value of 3000 are miscible over the whole composition and temperature range. A further increase of the molecular weights leads to immiscibility for blends with weight fractions of polystyrene more than 0.2 and less than 0.9 for  $M_w \geq 5600$  and less than 0.9 for  $M_w \geq 17\,500$ , respectively. The behavior is similar to that of the system poly( $\alpha$ -methylstyrene) (P $\alpha$ MS)/PS. However, the system PSi $\alpha$ MS/PS is miscible for lower molecular weights only. Obviously, the replacement of the quaternary carbon atom by a silicon atom leads to stronger repulsive interactions. The known miscibility behavior of P $\alpha$ MS/PS is described by the Patterson theory as well, in order to compare the interaction parameters of the two systems. Moreover, the temperature dependencies of the  $\chi$ -parameters of the two systems are compared using different expressions for  $\chi$  from three equation-of-state theories and based on the Gibbs free energy and the chemical potential. The Flory–Orwoll–Vrij theory, the Patterson theory, and the modified cell model of Dee and Walsh are employed. The interaction of P $\alpha$ MS/PS is more favorable to mixing than that of PSi $\alpha$ MS/PS. Finally, the experimentally observed immiscibility of PSi $\alpha$ MS with poly(2,6-dimethyl-1,4-phenylene oxide) and poly(vinyl methyl ether), respectively is explained in terms of the Patterson theory.

## Introduction

The binary polymer system poly( $\alpha$ -methylstyrene)/polystyrene (P $\alpha$ MS/PS) is known to be miscible for a certain range of molecular weights; for high molecular weights it is immiscible.<sup>1–13</sup> The known miscibility data are determined from cast films of ternary systems and inspection of their turbidity,<sup>6,8,11,13</sup> from  $T_g$  measurements,<sup>4–7,9,10,12,13</sup> and from small-angle neutron scattering.<sup>11</sup> The data obtained by thermal methods like DSC and DMA have to be taken while high heating rates are applied since P $\alpha$ MS shows vast thermal instability<sup>14</sup> and the measurement has to be finished before substantial depolymerization takes place. For the same reason, it is difficult to carry out cloud point measurements of films near or above  $T_g$  since the film should be annealed for a longer period of time in order to obtain equilibrium data. Thus, it is nearly impossible to carry out equilibrium measurements in the melt of the system P $\alpha$ MS/PS.

Poly(sila- $\alpha$ -methylstyrene) (PSi $\alpha$ MS) has better thermal stability than P $\alpha$ MS, and it differs from P $\alpha$ MS only by the replacement of the quaternary carbon atom by a silicon atom as shown in Figure 1. Thermogravimetry shows a thermal stability for PSi $\alpha$ MS up to a temperature of 300 °C.<sup>15</sup> On the one hand, considering the molecular constitution, the phase behavior of PSi $\alpha$ MS/PS blends might be similar to that of P $\alpha$ MS/PS and the above-mentioned problem concerning the thermal instability does not occur for this system. On the other hand, the van der Waals radii of carbon and silicon are so different that a measurable change in the blend behavior might be expected.

In this work, the miscibility of a PSi $\alpha$ MS with a number of PS samples having different molecular

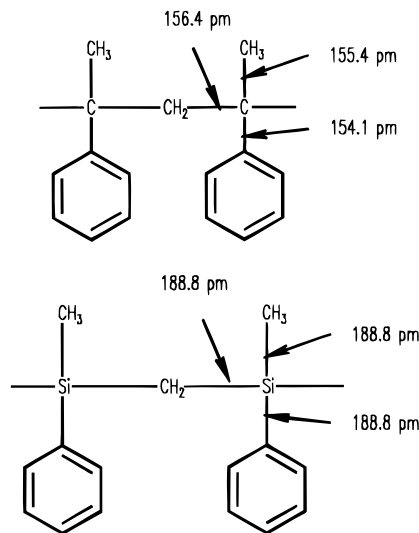


**Figure 1.** Comparison of the structures of P $\alpha$ MS and PSi $\alpha$ MS.

weights is studied by DSC and cloud point measurements. Then the observed miscibility behavior is interpreted by means of the Patterson equation-of-state (EOS) theory.<sup>16,17</sup> The same is done for the system P $\alpha$ MS/PS for miscibility data taken from the literature and compared with the system PSi $\alpha$ MS/PS. The temperature dependence of the interaction parameters,  $\chi$ , for the two systems is compared. The  $\chi$  values are calculated using the Patterson theory, the Flory–Orwoll–Vrij (FOV) theory,<sup>18,19</sup> and the modified cell model (MCM) of Dee and Walsh.<sup>20,21</sup> The expressions obtained from the Gibbs free energy and the chemical potential are compared. Finally, conclusions for the miscibility of PSi $\alpha$ MS with poly(vinyl methyl ether) (PVME) and poly(2,6-dimethyl-1,4-phenylene oxide) (PPO), respectively, are drawn from their EOS parameters.

\* To whom correspondence should be addressed.

<sup>⊗</sup> Abstract published in *Advance ACS Abstracts*, January 1, 1996.

## Theoretical Background

The miscibility of polymer blends can be described by a number of different thermodynamic theories, the most simple being the well-known Flory–Huggins (FH) theory.<sup>22–24</sup> Its free energy of mixing is given by

$$\Delta G = NrkT \left[ \frac{\Phi_1}{r_1} \ln \Phi_1 + \frac{\Phi_2}{r_2} \ln \Phi_2 + \chi \Phi_1 \Phi_2 \right] \quad (1)$$

where  $\Phi_i$  are volume fractions of polymers,  $r_i$  the numbers of segments per polymer chain, and  $N$  the number of molecules, and  $k$  is the Boltzmann constant. The sign and the temperature dependence of the interaction parameter  $\chi$ , appearing in this theory, gives information about the phase behavior of the blend. A binary mixture is stable when the following stability condition holds

$$2\chi < \frac{1}{r_1 \Phi_1} + \frac{1}{r_2 \Phi_2} \quad (2)$$

The more sophisticated EOS theories provide a more detailed insight into the thermodynamics of polymer blends. Their free energy also contains free-volume contributions, which are completely neglected by the incompressible FH theory. Since the simple FH theory is more easy to handle than the EOS theories, it is often used to extract the quantity  $\chi$  from EOS theories.

This is possible for example for the EOS theories that are based on the Prigogine ansatz.<sup>25,26</sup> In these theories, the size of a lattice site can be chosen arbitrarily, as for the FH theory. The  $\chi$ -parameter contains all contributions to the free energy of mixing that are not due to the combinatorial entropy. In the original Flory–Huggins theory,  $\chi$  is frequently assumed to be entirely of an enthalpic nature, but later an empirical entropic term was introduced to  $\chi$  by Guggenheim.<sup>27</sup> Using the more sophisticated EOS theories, an expression for  $\chi$  can be derived which a priori contains entropic contributions. However, there are different ways to determine  $\chi$  from these theories, and the results obtained may differ. One way is to equate the residual free energy of mixing (i.e., the terms that are not due to the combinatorial entropy) of the FH theory and the EOS theory and solve for  $\chi$ . The  $\chi$ -parameter obtained in this way then depends on composition. Another way is to equate the residual chemical potential of the FH theory and the EOS theory and also solve for  $\chi$ . The resulting  $\chi$ -parameter also depends on composition. The FH chemical potential is derived under the assumption of composition-independent  $\chi$ , and the  $\chi$ 's derived in the two ways described above depend on composition; therefore, the results differ.

In the EOS theories used in the present paper, a liquid is characterized by the reduction parameters  $p^*$ ,  $v_s^*$ , and  $T^*$ . These characteristic parameters have different numerical values for the different theories. Using these parameters, the reduced pressure, volume, and temperature ( $\tilde{p}$ ,  $\tilde{v}$ ,  $\tilde{T}$ ) are defined

$$\tilde{p} = \frac{p}{p^*}, \quad \tilde{v} = \frac{v_s}{v_s^*}, \quad \tilde{T} = \frac{T}{T^*} \quad (3)$$

where  $p$  is the pressure,  $v_s$  the specific volume, and  $T$  the temperature. Using the FOV theory, the  $\chi_{FG,tot}$ -parameter (for the meaning of all subscripts of the  $\chi$ -parameters see Appendix) obtained from equating the

Gibbs free energy of mixing of the EOS and FH theories reads

$$\chi_{FG,tot} = \frac{V_r^*}{\Phi_1 \Phi_2 RT} \left[ \Phi_1 p_1^* \left( \frac{1}{\tilde{v}_1} - \frac{1}{\tilde{v}} \right) + \Phi_2 p_2^* \left( \frac{1}{\tilde{v}_2} - \frac{1}{\tilde{v}} \right) + 3\Phi_1 p_1^* \tilde{T}_1 \ln \frac{\tilde{v}_1^{1/3} - 1}{\tilde{v}^{1/3} - 1} + 3\Phi_2 p_2^* \tilde{T}_2 \ln \frac{\tilde{v}_2^{1/3} - 1}{\tilde{v}^{1/3} - 1} + \frac{\Phi_1 \Theta_2 X_{12}}{\tilde{v}} \right] \quad (4)$$

where  $V_r^*$  is the molar hard-core volume of a segment taken as the reference volume.  $\Theta_2$  is the site fraction of the component 2, which is equal to the segment fraction, when the number of contact sites per segment is equal for both components. The first four terms of the right-hand side of eq 4 represent the free-volume part,  $\chi_{FG,fv}$  of the total interaction parameter  $\chi_{FG,tot}$ . They result from the derivation of the EOS theory, whereas the last term,  $\chi_{FG,int}$  is analogous to the  $\chi$ -parameter of the FH theory.

The MCM yields analogously

$$\chi_{MG,tot} = \frac{V_r^*}{\Phi_1 \Phi_2 RT} \left[ \Phi_1 p_1^* \left\{ A \left( \frac{1}{\tilde{v}_1^2} - \frac{1}{\tilde{v}^2} \right) - \frac{B}{2} \left( \frac{1}{\tilde{v}_1^4} - \frac{1}{\tilde{v}^4} \right) \right\} + \Phi_2 p_2^* \left\{ A \left( \frac{1}{\tilde{v}_2^2} - \frac{1}{\tilde{v}^2} \right) - \frac{B}{2} \left( \frac{1}{\tilde{v}_2^4} - \frac{1}{\tilde{v}^4} \right) \right\} + 3\Phi_1 p_1^* \tilde{T}_1 \ln \frac{\tilde{v}_1^{1/3} - 0.8909q}{\tilde{v}^{1/3} - 0.8909q} + 3\Phi_2 p_2^* \tilde{T}_2 \ln \frac{\tilde{v}_2^{1/3} - 0.8909q}{\tilde{v}^{1/3} - 0.8909q} + \Phi_1 \Theta_2 X_{12} \left( \frac{A}{\tilde{v}^2} - \frac{B}{2\tilde{v}^4} \right) \right] \quad (5)$$

where  $A$  and  $B$  are constants given by the geometry of the lattice. For a hexagonal close-packed geometry,  $A = 1.2045$  and  $B = 1.011$ .  $q$  was determined empirically to be 1.07. Again, the last term is equivalent to the FH  $\chi$ -parameter, and the others are due to the free volume.

Calculating the corresponding expressions from the residual chemical potential of component 1, the following expressions are obtained from FOV theory

$$\chi_{F\mu,tot} = \frac{V_r^* p_1^*}{RT} \left[ 3\tilde{T}_1 \ln \frac{\tilde{v}_1^{1/3} - 1}{\tilde{v}^{1/3} - 1} + \tilde{p}_1(\tilde{v} - \tilde{v}_1) + \left( \frac{1}{\tilde{v}_1} - \frac{1}{\tilde{v}} \right) + \frac{\Theta_2^2 X_{12}}{p_1^* \tilde{v}} \right] \quad (6)$$

and from MCM

$$\chi_{M\mu,tot} = \frac{V_r^* p_1^*}{RT} \left[ 3\tilde{T}_1 \ln \frac{\tilde{v}_1^{1/3} - 0.8909q}{\tilde{v}^{1/3} - 0.8909q} + \tilde{p}_1(\tilde{v} - \tilde{v}_1) + A \left( \frac{1}{\tilde{v}_1^2} - \frac{1}{\tilde{v}^2} \right) - \frac{B}{2} \left( \frac{1}{\tilde{v}_1^4} - \frac{1}{\tilde{v}^4} \right) + \frac{\Theta_2^2 X_{12}}{p_1^*} \left( \frac{A}{\tilde{v}^2} - \frac{B}{2\tilde{v}^4} \right) \right] \quad (7)$$

In eqs 4–7 the parameter  $X_{12}$  is a measure of the enthalpic interactions between the components and can be related to the classical  $\chi$ -parameter of the FH theory.

Taking the residual chemical potential of the Prigogine corresponding states theory,<sup>25,26</sup> a series expansion in the concentration has been performed by Patterson.<sup>16</sup>

**Table 1. Polymers Used, Their Properties and Sources**

polymer	abbrev	source	$M_w$	$M_w/M_n$	$T_g^a$ (°C)
polystyrene	PS-3k	Polymer Laboratories	3 000	1.1	80
polystyrene	PS-6k	Polymer Laboratories	5 600	1.12	94
polystyrene	PS-10k	Polymer Laboratories	10 300	1.06	98
polystyrene	PS-17k	Polymer Laboratories	17 500	1.06	99
polystyrene	PS-180k	Denka-Styrol	180 000	2.0	n.d. <sup>b</sup>
poly(sila- $\alpha$ -methylstyrene)	PSi $\alpha$ MS-188k	our laboratory	188 000	2.81	22
poly( $\alpha$ -methylstyrene)	P $\alpha$ MS-61k	our laboratory	61 000	1.04	170
poly(2,6-dimethylphenylene oxide)	PPO-31k	Aldrich	30 700	1.84	213
poly(vinylmethyl ether)	PVME-78k	Aldrich	78 000	1.62	n.d.

<sup>a</sup> Measured by DSC with a heating rate of 20 K/min. <sup>b</sup> Not determined.

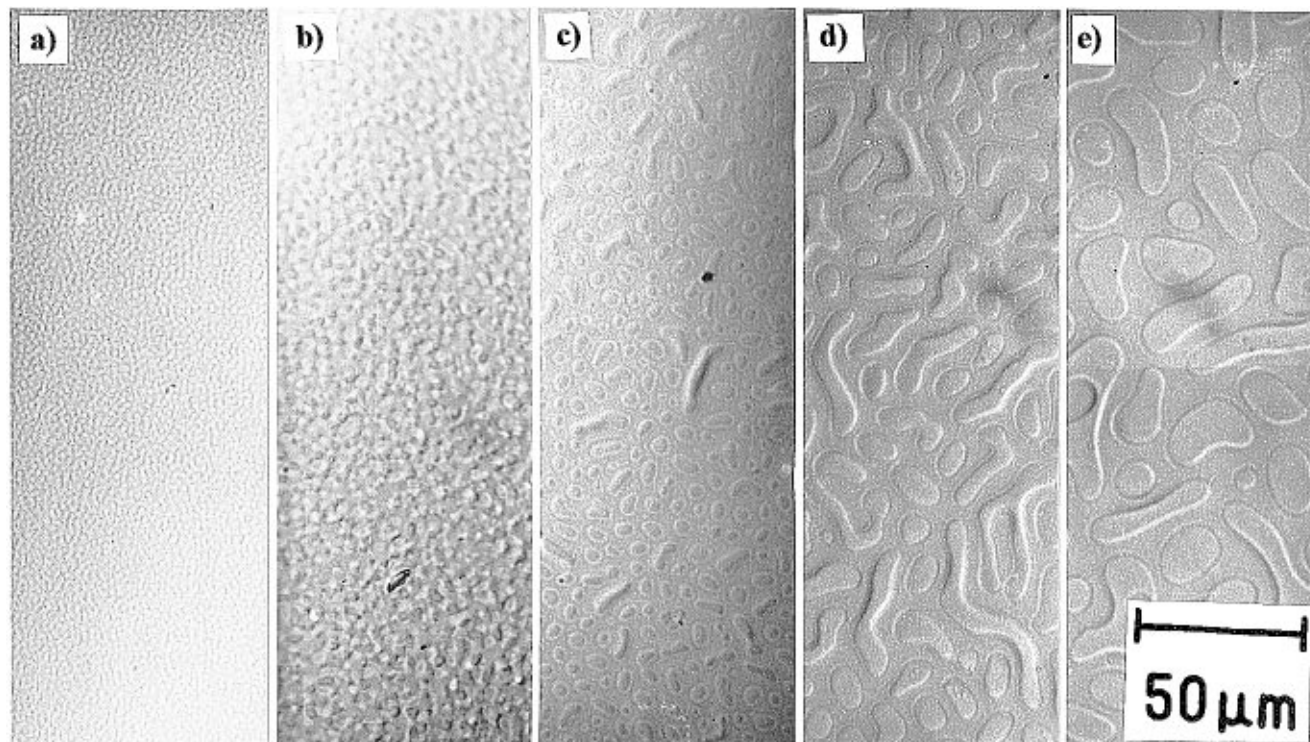


**Figure 2.** Light micrograph of a PSi $\alpha$ MS-188k/PS-6k 50/50 (wt %) sample after different times of isothermal annealing at 140 °C: (a) 2, (b) 5, (c) 10, (d) 30, and (e) 90 min.

This leads to a simple expression for the interaction parameter. Neglecting higher order terms, a concentration-independent  $\chi$ -parameter is obtained:

$$\chi_{P,tot} = -\frac{U_1 v^2}{RT} + \frac{C_{p1}}{2R} \left[ \tau + \frac{\kappa_1 P}{\alpha_1 T} \right]^2 \quad (8)$$

$\alpha_1$  and  $\kappa_1$  are expansion coefficient and compressibility, respectively, of component 1,  $U_1$  is the internal energy, and  $C_{p1}$  is the corresponding heat capacity.

Using the FOV theory, the quantity  $U_1$  reads

$$U_1 = -\frac{p_1^* V_1^*}{\tilde{v}_1} \quad (9)$$

$v^2$ ,  $\tau$ , and  $\pi$  are given by

$$v^2 = \frac{X_{12}}{p_1^*}, \quad \tau = 1 - \frac{T_1^*}{T_2^*}, \quad -\pi = 1 - \frac{p_1^*}{p_2^*} \quad (10)$$

The heat capacity  $C_{p1}$  is a function of  $p_1^*$ ,  $v_1^*$ ,  $T_1^*$ ,  $\tilde{p}_1$ , and  $\tilde{v}_1$ . In the expression for  $\chi$  of the Patterson theory, eq 8, the first term is the interactional one and the second the free-volume term.

## Experimental Section

**Materials.** The polymers used, their abbreviations, sources, molecular weight data, and glass transition temperatures are listed in Table 1.

**Preparation of Poly(methylphenylsilylenemethylene) (PSi $\alpha$ MS).** The PSi $\alpha$ MS was prepared by ring-opening polymerization of 1,3-dimethyl-1,3-diphenyl-1,3-disilacyclobutane using  $H_2PtCl_6$  as a catalyst.<sup>15</sup> Thermogravimetry showed a weight loss of 5% at 380 °C in air and at 470 °C in nitrogen. The heating rate was 5 °C/min.

**Blend Preparation and Cloud Point Measurements.** Different blend ratios of both polymers were dissolved in toluene at 80 °C (2 wt % of polymer total). The solution was then cast onto glass slides, and the solvent was evaporated at room temperature. These films were dried for several days. The as-cast films were isothermally annealed at 100 °C for several hours. The miscibility was judged by light microscopic inspection. It should be mentioned that the cloud point measurements have to be carried out very carefully. Figure 2 shows the development of the phase morphology during isothermal annealing at 140 °C of a PSi $\alpha$ MS/PS-6k 50/50 (wt %) blend. The initially transparent sample undergoes phase separation which could be assigned to an apparent LCST behavior. But annealing the same sample just above the  $T_g$  of PS leads also to phase separation. Because the as-cast film shows also two  $T_g$ 's, it can be assumed that the sample is immiscible and there does not exist a true LCST behavior.

**DSC Measurements.** The as-cast and dried films (approximately 10 mg) were placed into DSC pans. The samples were heated from -50 to 170 °C with 10 °C/min and then cooled to -50 °C using the same rate. The data were taken in the second run applying the same temperature regime. The measurements were carried out with a Perkin Elmer DSC-7.

**PVT Measurements.** The PVT measurements were performed with a Gnomix-PVT apparatus (Boulder, CO). The

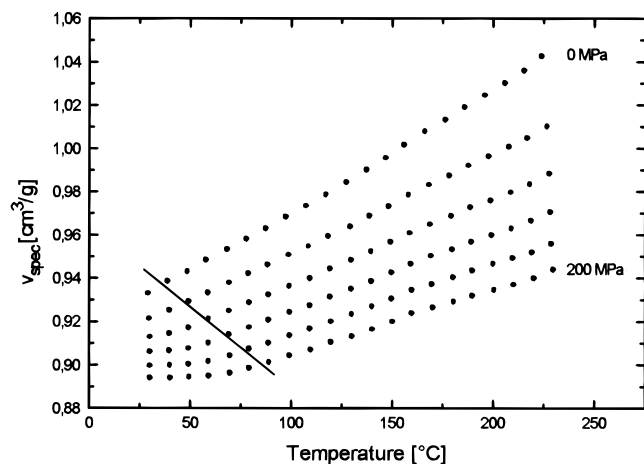


**Figure 3.** Isothermal PVT measurement of PSiMS. Isobars are shown from 0 to 200 MPa in intervals of 40 MPa. The solid line indicates the pressure-dependent glass transition temperature.

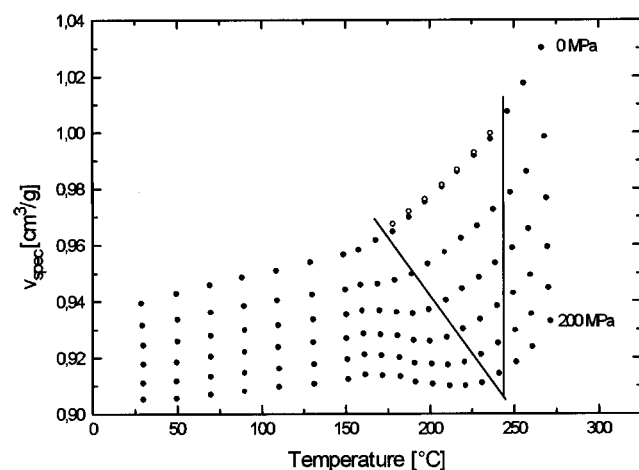


**Figure 4.** Isothermal PVT measurement of P $\alpha$ MS. Isobars are shown from 0 to 200 MPa in intervals of 40 MPa. The solid lines confine the data used for evaluation. The open circles represent the  $p = 0$  MPa data extrapolated by the PVT software. The solid circles in the  $p = 0$  MPa isobar were calculated by the MCM EOS.

sample cell contained about 1 g of polymer and mercury as a confining fluid. The apparatus has been described in detail elsewhere.<sup>28</sup> The measurements were performed in the isothermal mode, i.e., the sample was held at a certain temperature, and the pressure was continuously raised from 10 to 200 MPa with pressure, volume, and temperature being recorded in steps of 10 MPa. For PSiMS-188k, PS-180k, PS-6k, PPO-31k, and PVME-78k, the specific volume corresponding to  $p = 0$  MPa was extrapolated using the PVT software (Tait equation). Subsequently, this procedure was repeated for other temperatures. Figure 3 shows the PVT measurement of PSiMS. The solid line represents the pressure dependent  $T_g$ . The  $T_g$  is much lower compared to P $\alpha$ MS (about 170 °C at  $p = 0$  MPa), which is caused by the increased bond length of the Si-C bond in the main chain as shown in Figure 1.

The PVT measurement of P $\alpha$ MS can be seen in Figure 4. Again, the left solid line represents the border of the data that are influenced by the glass transition, whereas the right solid line separates the values that are obviously influenced by thermal degradation. For P $\alpha$ MS, the evaluation of the  $p = 0$  MPa data extrapolated by the Gnomix software (represented by the open circles in Figure 4) leads to unrealistic characteristic parameters, probably due to the thermal instability of this polymer (i.e., for example,  $p^*$  is increasing with increasing temperature instead of a decrease, which is usually observed<sup>29</sup>). The difficulties in obtaining reduction parameters of P $\alpha$ MS from PVT data were already reported by Quach and Simha.<sup>30</sup> Therefore, they were calculated using parametric

values characteristic of a given atom or atomic grouping.<sup>5,31</sup> The  $p = 0$  MPa data of P $\alpha$ MS used for our calculations were obtained by applying the EOS of the MCM theory. This theory describes the pressure dependence of the specific volume precisely even over large pressure ranges,<sup>32</sup> no matter whether the characteristic parameters were calculated at zero pressure or were fitted to the EOS. In order to compute the  $p = 0$  MPa data of P $\alpha$ MS, the melt data confined by the two solid lines were fitted to the MCM EOS, resulting in the following characteristic parameters:  $p^* = 708.5$  MPa,  $v_s^* = 0.8174$  cm<sup>3</sup>/g,  $T^* = 6701$  K. Using these parameters, the specific volume at  $p = 0$  MPa was calculated. These data, like the other PVT data of P $\alpha$ MS, are represented by the full circles in the  $p = 0$  isobar between 180 and 240 °C in Figure 4.

**Determination of the Reduction Parameters.** The characteristic parameters were determined for PSiMS-188k, P $\alpha$ MS-61k, PS-180k, and PS-6k, PPO-31k, and PVME-78k. For FOV theory, they were calculated at  $p = 0$  MPa from  $\alpha$ ,  $\kappa$ , and the specific volume, which were determined from the PVT data. For each polymer, only the melt data well above  $T_g$  were taken into account. Therefore, the characteristic parameters of each polymer could only be obtained for an individual temperature range. In order to account for the temperature dependence of the characteristic parameters,<sup>29</sup> linear regression was performed. Finally, the parameters of both components at  $T_g + 25$  °C ( $T_g$  of the neat high- $T_g$  component) were used for calculations. For MCM theory, the parameters were calculated from those of FOV theory as described elsewhere.<sup>32</sup> All parameters used for calculations are listed in Table 2.

## Results and Discussion

Although the EOS theories are in general not capable of predicting phase diagrams of polymer blends, they are extremely helpful to provide a physical interpretation of material parameters causing miscibility or immiscibility in polymer blends. For the description of the miscibility behavior of the systems under investigation, the Patterson theory is employed. Figure 5 shows the  $T_g$  as a function of the blend ratio of the system PSiMS-188k/PS for two different PS molecular weights. Blends of PSiMS-188k/PS-3k are completely miscible as indicated by the occurrence of a single composition-dependent glass transition temperature (Figure 5a). Blends containing PS-6k are already completely immiscible for all blend ratios measured (Figure 5b), except the blend containing 20 wt % PS-6k. The same result is obtained for blends containing PS-10k, whereas blends with PS-17k are completely immiscible for all blend compositions. Cloud point measurements are employed in order to judge the miscibility behavior. This is especially helpful for blends containing only 10 wt % of one of the components, where the DSC measurements are usually not sensitive enough. The miscibility of the samples is judged by microscopic inspection after isothermal annealing of the samples at 100 °C on a hot stage under nitrogen. Figure 6 shows some examples of the observed morphology for 50/50 (wt %) blends containing PS with different molecular weights. The blend of PSiMS-188k with PS-3k is completely transparent, and blends containing higher molecular weight PS samples show a two-phase morphology. It can be seen that morphologies are formed that resemble very much those of spinodal decomposition.<sup>33</sup> The size of the phases increases with increasing molecular weight of the PS.

The cloud point measurements were carried out for all blend ratios in steps of 10 wt %. The miscibility behavior of PSiMS-188k blends with PS of different molecular weights obtained from DSC and cloud point data is shown in Figure 7. The open symbols indicate miscibility, the full ones immiscibility. All DSC data are in agreement with cloud point measurements. The

Table 2. Reduction Parameters of the FOV Theory and MCM, Respectively

polymer	temp (°C)	FOV			MCM		
		$p^*$ (MPa)	$v_s^*$ (cm <sup>3</sup> /g)	$T^*$ (K)	$p^*$ (MPa)	$v_s^*$ (cm <sup>3</sup> /g)	$T^*$ (K)
PSiMS-188k	125	495.9	0.8232	8309	600.8	0.8447	6321
PS-6K	125	515.5	0.8475	7874	606.8	0.8684	5948
PS-180k	200	532.9	0.8271	8427	598.4	0.8475	6338
PαMS-61k	200	568.9	0.7964	8821	656.0	0.8166	6663
PPO-31k	240	468.7	0.8030	8340	497.9	0.8232	6256
PVME-78k	50	465.2	0.8095	6938	558.3	0.8280	5221

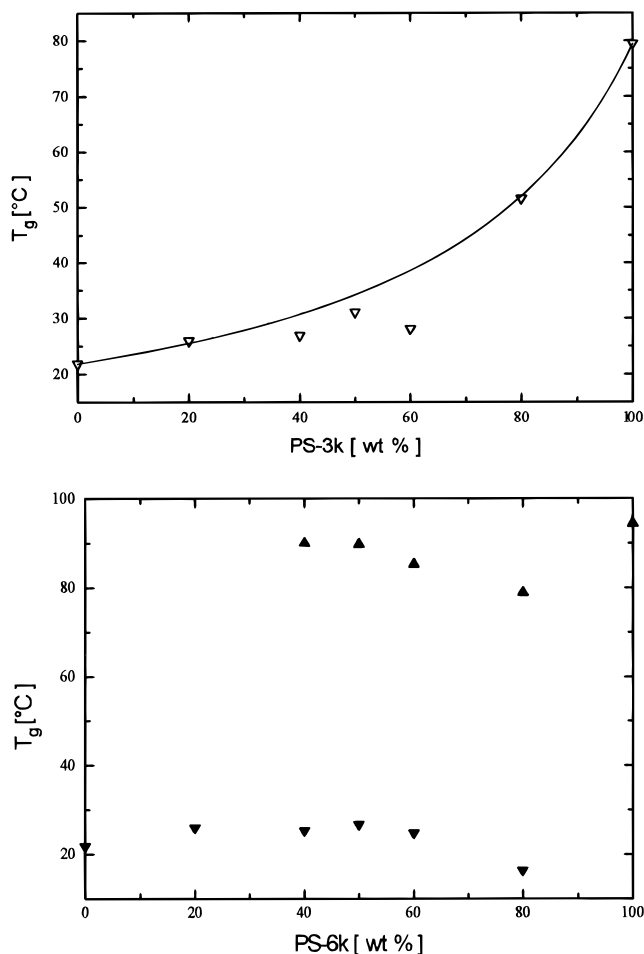


**Figure 5.** Glass transition versus blend composition for the systems (a, top) PS-3k/PSiMS (the full line is obtained using the Fox equation) and (b, bottom) PS-6k/PSiMS.

solid line represents the binodal points at 100 °C taken from calculated phase diagrams for the blends of PSiMS-188k with PS of different molecular weights. The phase diagrams were calculated using the characteristic parameters of PSiMS-188k and PS-6k at 125 °C. The parameter  $X_{12}$ , discussed under Theoretical Background, was fitted to calculate the miscibility of the PSiMS-188k blends with PS as a function of molecular weight in terms of the Patterson theory. For the description of the observed miscibility behavior, a value of  $X_{12} = 0.5$  J/cm<sup>3</sup> was required. It should be mentioned that the calculated phase diagrams show only upper critical solution temperature (UCST) behavior.

The miscibility behavior of blends of PαMS with PS has been studied by various techniques as already discussed. On the one hand, many miscibility data were obtained from blends precipitated from ternary solutions using different solvents without further annealing above  $T_g$ . This is because the equilibrium phase diagrams in the melt are hard to obtain because of the thermal instability of PαMS. The results obtained in this way

may deviate from the thermodynamic equilibrium and are difficult to compare with each other. On the other hand, there is only one data set,<sup>4</sup> as far as the authors are concerned, taken from DSC measurements of binary blends, varying the molecular weight and weight fraction of PS systematically and fixing the molecular weight of PαMS. In Figure 8, these experimental points are shown, where the molecular weight of PαMS is  $M_w = 90\,000$ . Again, the open symbols indicate miscibility, the full ones immiscibility. The binodal points resulting in the solid line are taken from phase diagrams of blends of PαMS with PS of different molecular weights at 175 °C. For the calculation, the characteristic parameters of PαMS-61k and PS-180k at 200 °C were used. A value of  $X_{12} = 0.048$  J/cm<sup>3</sup> is required to describe the miscibility behavior. USCT and LCST behavior are found up to PS molecular weights of 37 400 (PαMS fixed to be 90 000 g/mol). For higher molecular weights, the typical "hourglass" behavior is found.<sup>34</sup> The  $X_{12}$  value is adjusted to give binodal values just above the three data points for miscible blends. Applying a larger  $X_{12}$  value would shift the solid line toward lower molecular weights, which would be in disagreement with the experiments. Thus, an  $X_{12}$  value of 0.048 J/cm<sup>3</sup> yields the maximum repulsive enthalpic interactions possible. Use of this  $X_{12}$  value also yields binodal curves describing the experimental results obtained by Widmaier and Mignard.<sup>7</sup>

Having the values of the parameter  $X_{12}$  and the EOS parameters, it is possible to calculate the total  $\chi$ -parameters as a function of temperature for the Patterson and FOV theories. For the calculation with the latter theory a volume fraction of PS,  $\Phi_{PS} = 0.5$ , was used. The molar hard-core volume of a segment  $V_r^*$  was chosen to be 100 cm<sup>3</sup>/mol. Figure 9 shows the contributions of the interactions to the  $\chi$ -parameter,  $\chi_{x,int}$ , the contributions of the free-volume part  $\chi_{x,fv}$ , and the total value  $\chi_{x,tot}$  of the  $\chi$ -parameter of the system PSiMS-188k/PS. It can be seen that all values obtained from Patterson theory and FOV theory differ only marginally. Also, interaction parameters calculated from the Gibbs free energy and the chemical potential of the FOV theory (eqs 4 and 6) are nearly identical. Caused by very similar expansion coefficients, the free-volume contribution to the overall interaction parameter is extremely small. This is documented in the Patterson  $\tau$ -parameter (eq 10), which is  $|\tau| = 0.055$ . Thus, it is reasonable that according to the classical FH theory only UCST behavior can be observed; i.e., the total interaction parameter decreases monotonically with increasing temperature. This is caused by the reduction of unfavorable enthalpic interactions documented in the decrease of  $\chi_{x,int}$  with increasing temperature. Describing  $\chi_{P,tot}$  as  $a + b/T$  yields the parameters  $a = 0.0032$  and  $b = 5.46$  K. Figure 10 shows the interaction parameters obtained by the MCM. Again, the value of  $\Phi_{PS}$  was 0.5. In order to yield the same value of the  $\chi_{x,tot}$ -parameter obtained by the Patterson and FOV theories at a temperature of 100 °C, a  $X_{12}$  value of 0.63 J/cm<sup>3</sup> had to be used. The data of the Patterson theory are added

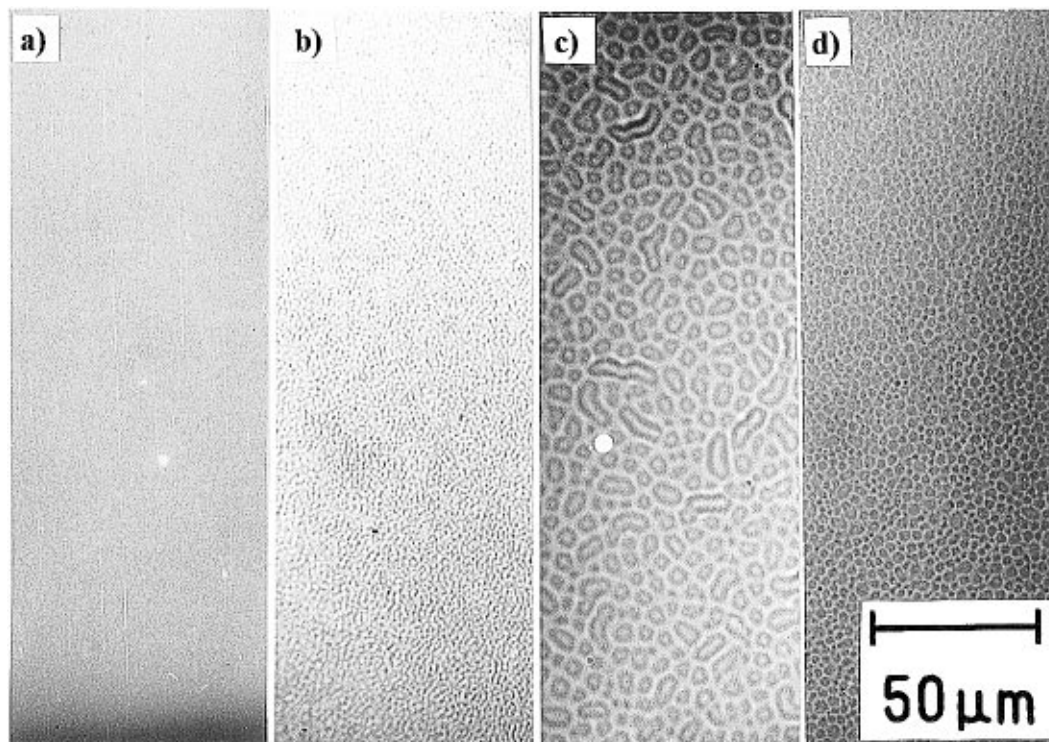


**Figure 6.** Light micrographs of the phase morphology of 50/50 (wt %) blends of PSi $\alpha$ MS-188k/PS annealed for 5 min at 100 °C with different PS molecular weights ( $M_w$ ): (a) 3000, (b) 5600, (c) 10 300, and (d) 17 500.

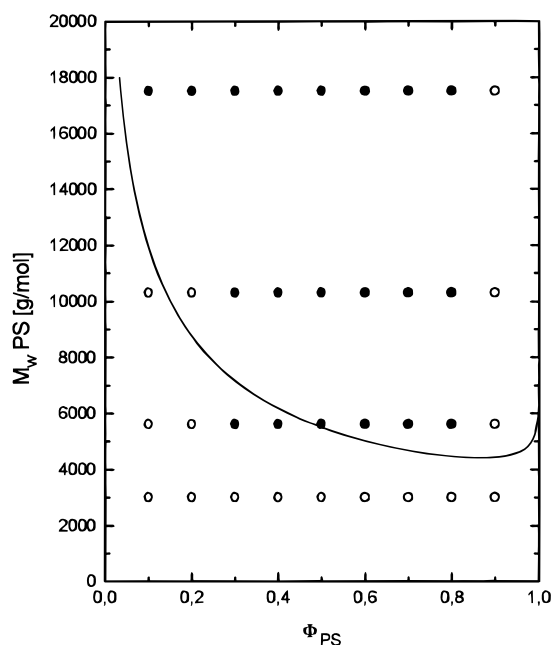


**Figure 7.** Miscible and immiscible blends in the system PS/PSi $\alpha$ MS as a function of blend ratio and molecular weight of PS. The  $M_w$  value PSi $\alpha$ MS is 188 000: (○) miscible; (●) immiscible. The full line is calculated (see text).

for the sake of comparison. Again, all theories yield similar values and it does not matter if the equations for the Gibbs free energy or for the chemical potential are used (eqs 4 and 5 or 6 and 7, respectively). Also, this theory predicts exclusively UCST behavior. From all calculations, it can be considered that the phase behavior of the system PSi $\alpha$ MS/PS is mainly governed by enthalpic interactions and their temperature dependence, whereas free-volume contributions are of minor influence.

The situation is completely different for the system P $\alpha$ MS/PS. Figure 11 depicts the temperature dependence of various interaction parameters obtained by the

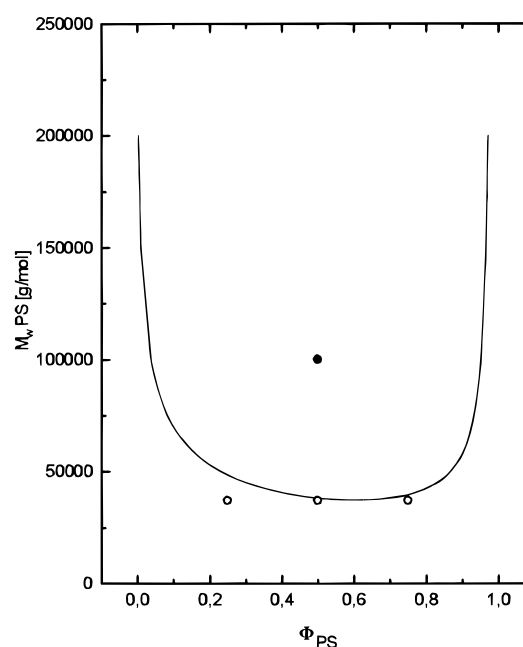


**Figure 8.** Miscible and immiscible blends in the system PS/P $\alpha$ MS as a function of blend ratio and molecular weight of PS. The  $M_w$  value P $\alpha$ MS is 90 000: (○) miscible, (●) immiscible. The full line is calculated (see text).

Patterson and FOV theories. It should be noted that all values of  $\chi_{x,int}$  are 1 order of magnitude smaller than in the system PSi $\alpha$ MS/PS. It is significant that the contributions of the free volume to the total interaction parameter in the system P $\alpha$ MS/PS are larger than the enthalpic contributions, although the absolute values of  $\chi_{x,fv}$  are similar for both systems ( $|\tau| = 0.047$  for P $\alpha$ MS/PS). Thus, the main difference between both systems is the stronger repulsive interactions in the system PSi $\alpha$ MS/PS compared to P $\alpha$ MS/PS. This is indicated by the  $X_{12}$  values. The small value of  $X_{12} = 0.048$  J/cm<sup>3</sup> means that blends of P $\alpha$ MS/PS are nearly athermal whereas an  $X_{12}$  value of 0.5 J/cm<sup>3</sup> for the

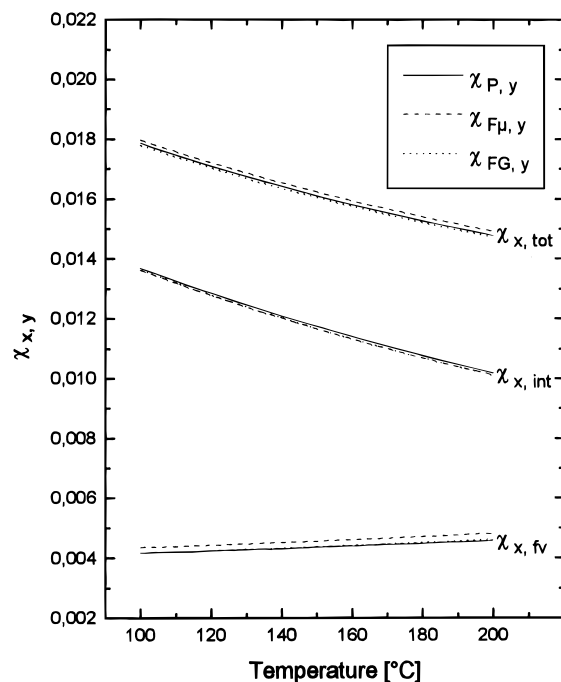


**Figure 9.**  $\chi_{\text{tot}}$ ,  $\chi_{\text{int}}$ , and  $\chi_{\text{fv}}$  for the system PS/PS $\alpha$ MS calculated by the Patterson and FOV theories. For FOV, the  $\chi$ -values were calculated from the chemical potential and from the free energy.

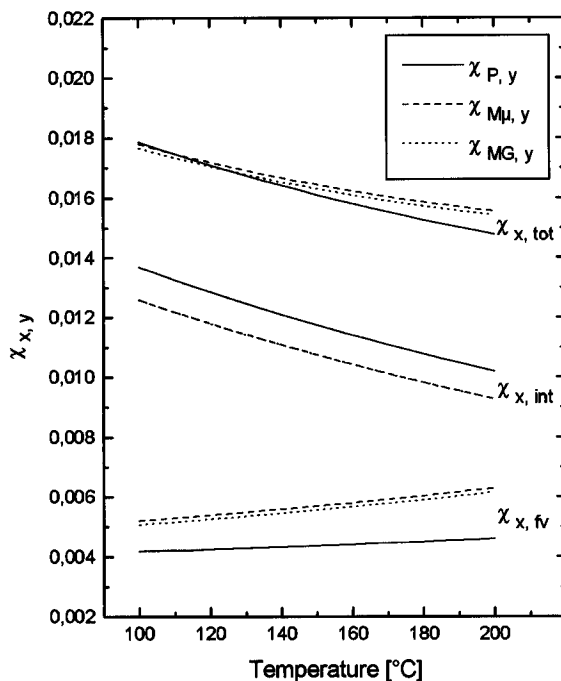


**Figure 10.**  $\chi_{\text{tot}}$ ,  $\chi_{\text{int}}$ , and  $\chi_{\text{fv}}$  for the system PS/PS $\alpha$ MS calculated by the MCM theory. For MCM, the  $\chi$ -values were calculated from the chemical potential and from the free energy. The Patterson data are added for comparison.

system PS $\alpha$ MS/PS documents that strong positive enthalpic interactions are present. It is interesting to note that the relative contribution of the free-volume part to the total interaction parameter has a dominant influence on the phase behavior in this blend system. The total interaction parameter is nearly temperature independent according to Patterson and FOV theories and is in excellent agreement with the  $\chi$ -value of 0.005 determined by small-angle neutron scattering.<sup>11</sup> Using the MCM theory, where  $X_{12}$  is equal to 0.057 J/cm<sup>3</sup>, results in a larger contribution of the free volume to the total interaction parameter. Thus, this parameter

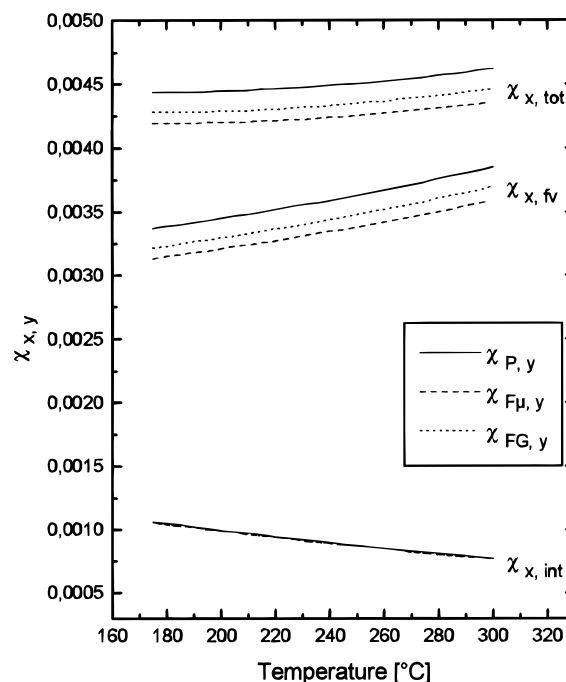


**Figure 11.**  $\chi_{\text{tot}}$ ,  $\chi_{\text{int}}$ , and  $\chi_{\text{fv}}$  for the system PS/P $\alpha$ MS calculated by the Patterson and FOV theories. For FOV, the  $\chi$ -values were calculated from the chemical potential and from the free energy.

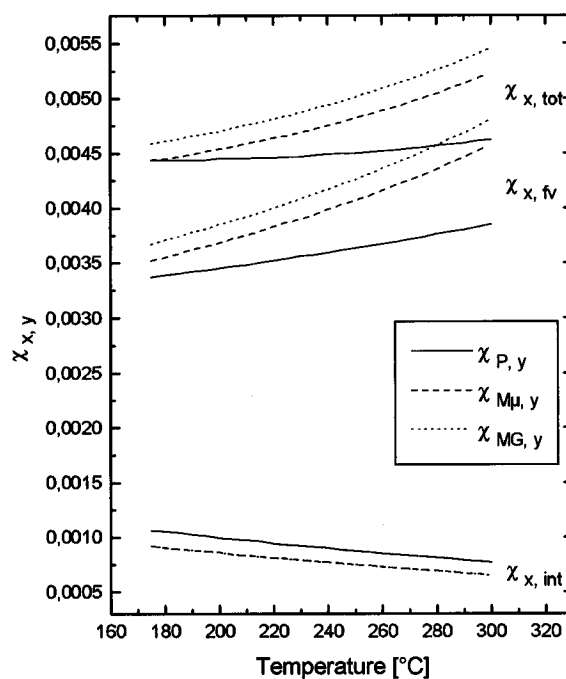


**Figure 12.**  $\chi_{\text{tot}}$ ,  $\chi_{\text{int}}$ , and  $\chi_{\text{fv}}$  for the system PS/P $\alpha$ MS calculated by the MCM theory. For MCM, the  $\chi$ -values were calculated from the chemical potential and from the free energy. The Patterson data are added for comparison.

increases with increasing temperature (see Figure 12). The total interaction parameter is increasing over the whole temperature range, at least providing the possibility of the occurrence of LCST behavior.

Furthermore, it has been known that PPO is miscible with PS,<sup>35,36</sup> P $\alpha$ MS,<sup>2,37</sup> and random copolymers of styrene and  $\alpha$ -methylstyrene<sup>38</sup> at all blend compositions, temperatures and molecular weights. Replacement of the quaternary carbon atom by silicon leads to complete immiscibility as shown in Figure 13. All blend compositions have two glass transitions near to those of the neat components. This immiscibility cannot be caused by



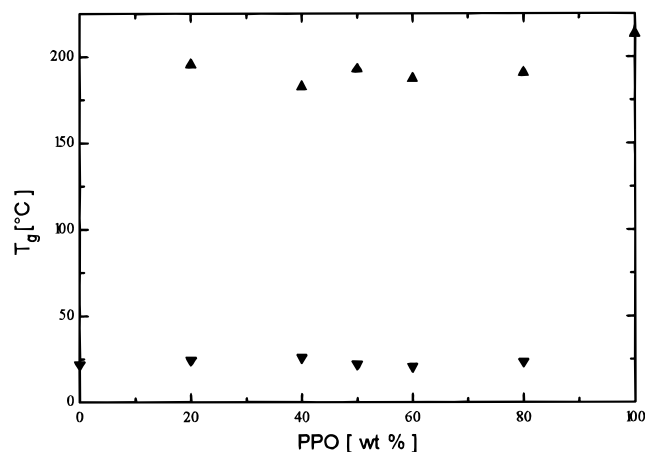


**Figure 13.** Glass transition versus blend composition for the system PPO-31K/PSi $\alpha$ MS-188k.

free-volume effects only, because the thermal expansion coefficients of PPO and PSi $\alpha$ MS are similar, resulting in  $|\tau| = 0.072$  at 240 °C. Again, the more unfavorable enthalpic interactions must be responsible. Blends of PVME with PSi $\alpha$ MS having high molecular weights as indicated in Table 1 are also completely immiscible. In this case, the value  $|\tau| = 0.139$  is bigger compared to the other systems, indicating also larger free-volume contributions to  $\chi_{x,\text{tot}}$ .

## Conclusions

It has been shown that the replacement of a quaternary carbon atom in P $\alpha$ MS by a silicon atom leads to more unfavorable interactions when PSi $\alpha$ MS is mixed with PS. Thus, the system PSi $\alpha$ MS/PS is miscible only for lower molecular weights compared to the system P $\alpha$ MS/PS. An EOS analysis shows that free-volume effects are negligible in the system PSi $\alpha$ MS/PS because the repulsive interactions are dominant. Therefore, only UCST behavior can be calculated for this system. The situation is different for the system P $\alpha$ MS/PS. Here the free-volume effect and the interactions are of the same order of magnitude because these blends are nearly athermal. It also appears that LCST behavior might occur in this system. Finally, it has been demonstrated that PSi $\alpha$ MS-188k is immiscible with PPO-31k and PVME-78k, respectively.

**Acknowledgment.** We are grateful to Axel Eckstein for providing the poly( $\alpha$ -methylstyrene)-61k sample.

## Appendix

The subscripts of the various  $\chi$ -parameters have the following meaning:  $\chi_F$ ,  $\chi_M$ , and  $\chi_P$  refer to the theory used for calculations, i.e., Flory–Orwoll–Vrij, Modified cell model, and Patterson. The subscripts “G” and “ $\mu$ ” stand for the use of the expressions obtained from the Gibbs free energy and the chemical potential, respectively. For the Patterson theory, this subscript is not

necessary, because it refers always to the chemical potential. The subscripts “tot”, “fv”, and “int” are related to the overall  $\chi$ -parameter, the free-volume contribution, and the contributions of interactions to the  $\chi$ -parameter, respectively.

## References and Notes

- (1) Dunn, D. J.; Krause, S. *J. Polym. Sci., Polym. Lett. Ed.* **1974**, *12*, 591.
- (2) Robeson, L. M.; Matzner, M.; Fetters, L. J.; McGrath, J. E. In *Recent Advances in Polymer Blends, Grafts and Blocks*; Sperling, L. H., Ed.; Plenum Press: New York, 1974; pp 281–300.
- (3) Krause, S. In *Polymer Blends*; Burke, J. J., Newman, S., Eds.; Academic Press: New York, 1978; Vol. 1, Chapter 2, pp 15–113.
- (4) Lau, S. F.; Pathak, J.; Wunderlich, B. *Macromolecules* **1982**, *15*, 1278.
- (5) Saeiki, S.; Cowie, J. M. G.; Mc Ewen, I. J. *Polymer* **1983**, *24*, 60.
- (6) Cowie, J. M. G.; Mc Ewen, I. J. *Polymer* **1985**, *26*, 1667.
- (7) Widmaier, J. M.; Mignard, G. *Eur. Polym. J.* **1987**, *23*, 989.
- (8) Lin, J.-L.; Roe, R.-J. *Macromolecules* **1987**, *20*, 2168.
- (9) Lin, J.-L.; Roe, R.-J. *Polymer* **1988**, *29*, 1227.
- (10) Schneider, H. A.; Dilger, P. *Polym. Bull.* **1989**, *21*, 265.
- (11) Rameau, A.; Gallot, Y.; Marie, P.; Farnoux, B. *Polymer* **1989**, *30*, 386.
- (12) Yang, H.; Ricci, S.; Collins, M. *Macromolecules* **1991**, *24*, 5218.
- (13) Callaghan, T. A.; Paul, D. R. *Macromolecules* **1993**, *26*, 2439.
- (14) Kilroe, J. G.; Weale, K. E. *J. Chem. Soc.* **1960**, 3849.
- (15) Koopmann, F.; Burgath, A.; Knischka, R.; Leukel, J.; Frey, H.; Mülhaupt, R. in preparation.
- (16) Patterson, D. *J. Polym. Sci. Part C* **1968**, *16*, 3379.
- (17) Patterson, D.; Robard, A. *Macromolecules* **1978**, *11*, 690.
- (18) Flory, P. J.; Orwoll, R. A.; Vrij, A. *J. Am. Chem. Soc.* **1964**, *86*, 3507.
- (19) Flory, P. J.; Orwoll, R. A.; Vrij, A. *J. Am. Chem. Soc.* **1964**, *86*, 3515.
- (20) Dee, G. T.; Walsh, D. J. *Macromolecules* **1988**, *21*, 811.
- (21) Dee, G. T.; Walsh, D. J. *Macromolecules* **1988**, *21*, 815.
- (22) Flory, P. J. *J. Chem. Phys.* **1941**, *9*, 660.
- (23) Huggins, M. L. *Ann. N.Y. Acad. Sci.* **1942**, *43*, 1.
- (24) Huggins, M. L. *J. Phys. Chem.* **1942**, *46*, 151.
- (25) Prigogine, I. *The Molecular Theory of Solutions*; North-Holland: Amsterdam, 1959.
- (26) Prigogine, I.; Trappeniers, N.; Mathot, V. *Discuss. Faraday Soc.* **1953**, *15*, 93.
- (27) Guggenheim, E. A. *Discuss. Faraday Soc.* **1953**, *15*, 24.
- (28) Zoller, P.; Bolli, P.; Pahud, V.; Ackermann, H. *Rev. Sci. Instrum.* **1976**, *47*, 948.
- (29) Sanchez, I. C. In *Polymer Blends*; Burke, J. J., Newman, S., Eds.; Academic Press: New York, 1978; Vol. 1, Chapter 3, pp 115–139.
- (30) Quach, A.; Simha, R. *J. Appl. Phys.* **1971**, *42*, 4592.
- (31) Manzini, G.; Crescenzi, V. *Gazz. Chim. Ital.* **1974**, *104*, 51.
- (32) Rudolf, B.; Kressler, J.; Shimomai, K.; Ougizawa, T.; Inoue, T. *Acta Polym.* **1995**, *46*, 312.
- (33) Hashimoto, T. Structure of Polymer Blends. In *Materials Science and Technology*; Thomas, E. L., Ed.; Verlag Chemie: Weinheim, 1993; Vol. 12.
- (34) McMaster, L. P. *Macromolecules* **1973**, *6*, 760.
- (35) Shultz, A. R.; Gendron, B. M. *J. Appl. Polym. Sci.* **1972**, *16*, 461.
- (36) Alexandrovich, P.; Karasz, F. E.; MacKnight, W. J. *J. Appl. Phys.* **1976**, *47*, 4251.
- (37) Kressler, J.; Kammer, H. W.; Herzog, K.; Heyde, H. *Acta Polym.* **1990**, *41*, 1.
- (38) Shultz, A. R.; Young, A. L. *J. Appl. Polym. Sci.* **1983**, *28*, 1677.

MA951296+